Journal of Medicinal Chemistry

ARTICLE

pubs.acs.org/jmc

Identification of 3*H*-Naphtho[1,2,3-*de*]quinoline-2,7-diones as Inhibitors of Apoptosis Signal-Regulating Kinase 1 (ASK1)

Galyna P. Volynets,[†] Maksym O. Chekanov,[†,‡] Anatoliy R. Synyugin,[†,‡] Andriy G. Golub,[†] Oleksandr P. Kukharenko,[†] Volodymyr G. Bdzhola,[†] and Sergiy M. Yarmoluk*[,†,‡]

[†]Institute of Molecular Biology and Genetics, NAS of Ukraine, 150 Zabolotnogo Str., 03143, Kyiv, Ukraine

[‡]Otava, Ltd., 150 Zabolotnogo Str., 03143, Kyiv, Ukraine

ABSTRACT: Apoptosis signal-regulating kinase 1 (ASK1) has recently emerged as an attractive therapeutic target for the treatment of cardiac and neurodegenerative disorders. The selective inhibitors of ASK1 may become important compounds for the development of clinical agents. We have identified the ASK1 inhibitor among 3*H*-naphtho[1,2,3-*de*]quinoline-2,7-diones using receptor-based virtual screening. In vitro kinase assay revealed that ethyl 2,7-dioxo-2,7-dihydro-3*H*-naphtho[1,2,3-*de*]quinoline-1-carboxylate (NQDI-1) inhibited ASK1 with a K_i of 500 nM. The competitive character of inhibition is demonstrated in Lineweaver−Burk plots. In our preliminary selectivity study this compound exhibited strong specific inhibitory activity toward ASK1.

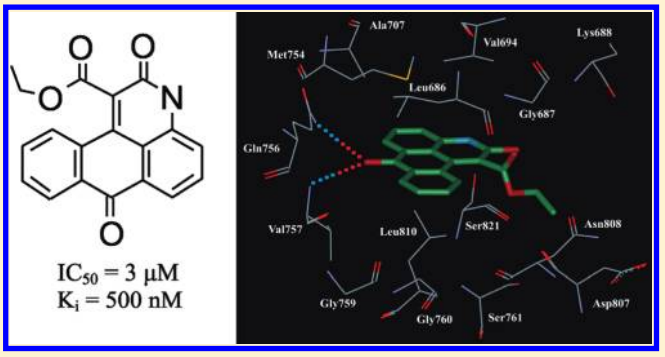

INTRODUCTION

Apoptosis signal-regulating kinase 1 (ASK1) is the ubiquitously expressed mitogen-activated protein kinase kinase kinase 5 that has a broad range of biological functions depending on the cell type and cellular context. ASK1 is associated with several diseases and may be a target for pharmaceutical intervention. For example, ASK1 was identified as an essential component in the neuronal death signaling pathway induced by expanded polyglutamine (polyQ) repeats.[1] Reactive oxygen species (ROS) mediated ASK1 activation by amyloid β (Aβ) protein is an important step in Alzheimer's disease pathogenesis.[2] Recently, it has been revealed that ASK1 is also involved in motor neuron cell death during familial amyotrophic lateral sclerosis.[3] Therefore, inhibitors of ASK1 can be considered as therapeutic remedies for patients with chronic neurodegenerative diseases.

New experimental results clearly showed that ASK1 deficiency attenuated cardiac inflammation and fibrosis, as well as vascular endothelial dysfunction and remodeling induced by the obesity/diabetes. ASK1 deficiency also abolished hepatic steatosis in diabetic mice.[4] Moreover, the inhibition of ASK1 by the recombinant adeno-associated virus expressing a dominant-negative ASK1ΔN-KR mutant was capable of suppressing heart failure progression by preventing cardiomyocyte apoptosis.[5] Hence, the inhibition of ASK1 activity may provide a valid approach for the treatment of cardiovascular diseases. In addition, ASK1 inhibitors could have broad therapeutic potential for many acute syndromes such as cardiac infarction or stroke as inhibitors of apoptosis.

In vivo study supports the role of ASK1 in the immune response, since ASK1-deficient mice were resistant to lipopolysaccharide (LPS) induced septic shock.[6] ASK1 can also be regarded as an important therapeutic target for the treatment of malignant fibrous histiocytoma.[7]

Thus, the potent and selective inhibitors of ASK1 would be important compounds for the development of clinical agents. However, there have been few reports regarding ASK1 inhibitors.[8−10] The main aim of our research is to identify the small molecule inhibitors of ASK1.

RESULTS AND DISCUSSION

The in silico approach is an important part of protein kinase inhibitor rational design. The docking process involves the prediction of ligand conformation within a targeted binding site and energy calculations (electrostatic and van der Waals) during complex formation.[11] The most important application of docking software is a virtual screening that allows selection of the most interesting and promising molecules from the existing compound collections for further evaluation and investigation.

In order to discover novel ASK1 inhibitors, we have performed a screening program, using both in silico and in vitro approaches. The system based on DOCK 4.0 package was used for receptor−ligand flexible docking.[12−15] The virtual screening experiments were carried out targeting the ATP binding site of ASK1 by browsing the commercially available compound library of 156 000 organic compounds.[16] The most promising 172 compounds having a docking score less than −50 kcal/mol have been selected and taken for the kinase assay study. In vitro experiments revealed that ethyl 2,7-dioxo-2,7-dihydro-3*H*-naphtho

Received: November 10, 2010
Published: March 30, 2011

dx.doi.org/10.1021/jm200117h | *J. Med. Chem.* 2011, 54, 2680–2686

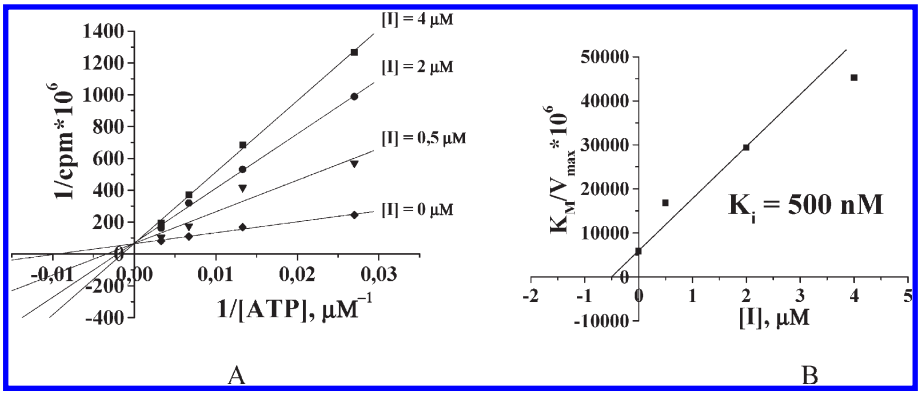

Figure 1. Kinetic analysis of **1**—ASK1 complexation consistent with a reversible and competitive mechanism of inhibition. ASK1 activity was determined as described in the Experimental Section either in the absence or in the presence of the indicated concentrations. The data represent the mean of triplicate experiments with SEM never exceeding 15%. (A) Lineweaver—Burk linearized plots of the substrate concentration curves for ASK1 at different concentrations of the compound **1**. Concentration of inhibitor varied from 0 to 4 μM. (B) Calculation of K_i from linear regression analysis of Lineweaver—Burk double-reciprocal plots.

Table 1. Residual Activity of Protein Kinases (%) in the Presence of 1 at 25 μM[a]

ASK1	Aurora A	ROCK	HGFR	FGFR1	Tie2	JNK3	CK2
12.5	79	100	62	44	84	100	78

[a] The values of residual activity represent the mean of at least three independent experiments with SEM never exceeding 15%. Final concentration of ATP in the experiment was 100 μM.

[1,2,3-*de*]quinoline-1-carboxylate (NQDI-1) inhibited ASK1 with an IC_{50} of 3 μM.

The Lineweaver—Burk plots, which are the linearized transformations of the Michaelis—Menten curves, demonstrate the competitive character of inhibition for compound **1** (NQDI-1), as the inhibitor decreases K_M without affecting V_{max} (Figure 1A). K_i of 500 nM has been calculated from linear regression analysis of Lineweaver—Burk double reciprocal plots (Figure 1B).

The selectivity of **1** was evaluated in vitro on four serine/threonine protein kinases (protein kinase CK2 (CK2), c-Jun N-terminal kinase 3 (JNK3), Rho-associated protein kinase 1 (Rock1), and Aurora A) and three tyrosine protein kinases (fibroblast growth factor receptor 1 (FGFR1), hepatocyte growth factor receptor (HGFR), and endothelial TEK tyrosine kinase (Tie2)). The results of our study have shown that **1** seems to be a selective inhibitor of ASK1 (Table 1). The activity of FGFR1 protein kinase is inhibited by **1** (residual activity of 44%); nevertheless, we suppose that this derivative of 3*H*-naphtho[1,2,3-*de*]quinoline-2,7-dione is a promising lead for extended selectivity evaluation and optimization.

In order to examine the structure—activity relationships of the derivatives of 3*H*-naphtho[1,2,3-*de*]quinoline-2,7-dione, the structural analogues were selected from the Otava, Ltd. compound library and tested in vitro.

Several important structural features of 3*H*-naphtho[1,2,3-*de*]quinoline-2,7-dione derivatives can be identified from a qualitative analysis of their activity on ASK1 (Table 2). The ASK1 inhibitory activity of the studied derivatives depends on the nature of R^1 substituents in this heterocyclic system. The most active compound **1** with R^1 = acetic acid ethyl ester has IC_{50} = 3 μM. The presence of an acetyl group in this position has a negative effect on the inhibitory activity of derivative **4** (IC_{50} = 15 μM). Compound **2**, wherein R^1 is a methylamine, has IC_{50} = 4.7 μM. Compound **3** with ethylamine in this position has IC_{50} = 10 μM, and compounds **5** and **6** substituted with 2-hydroxyethylamine and benzoyl have IC_{50} equal to 25 and 35 μM, respectively.

The nature of the R^3 substituent also significantly affects the inhibitory activity toward ASK1. For instance, in derivative **4** (IC_{50} = 15 μM), a substitution of the hydrogen atom with a methyl group (derivative **7**) results in over 2-fold decrease in activity (IC_{50} = 35 μM)).

The R^4 substituent of the scaffold is of special interest. All active compounds have hydrogen in this position. The substitution of hydrogen atom with any other chemical groups results in a complete loss of inhibition efficiency (derivatives **8**—**15**).

The compounds in this class are reversible ATP-competitive inhibitors of ASK1 and, as expected, occupy the ATP binding region between the N-terminal and C-terminal lobes of the ASK1 enzyme. Our molecular docking investigations have demonstrated that active derivatives of 3*H*-naphtho[1,2,3-*de*]quinoline-2,7-dione display a very good steric and chemical complementarity with the ATP-binding pocket. Apolar interactions with hydrophobic residues Leu686, Val694, Ala707, Met754, Val757, Gly759, and Gly760 are the most important noncovalent forces that contribute to the ligand recognition process. A peculiarity of the active inhibitor binding mode in comparison to those displayed by other investigated compounds is the formation of a hydrogen bond with Val757 in the hinge region. All active compounds (**1**—**7**) have R^4 = H, whereas all the nonactive compounds have various substituents in this position adjacent to the carbonyl group. The substitution of the hydrogen atom with any other chemical group results in a complete loss of inhibition efficiency (derivatives **8**—**15**). According to the visual inspection of the complexes obtained with docking, R^4 = H allows formation of hydrogen bonds with Val757 in the hinge region for compounds **1**—**7**, while all the inactive compounds do not form this hydrogen bond. The loss of the activity may be explained as due to the introduction of steric hindrance into this area of the binding pocket that, in consequence, results in destabilization of the ligand in the ASK1 active site.

Since the protein molecule remains rigid during the docking, we performed a 10 ns molecular dynamics (MD) simulation to more accurately predict the binding mode of **1** with the ATP-binding site of protein kinase ASK1. The binding mode calculated with MD is similar to the one obtained with docking, and

dx.doi.org/10.1021/jm200117h |*J. Med. Chem.* 2011, 54, 2680–2686

Table 2. Structures and in Vitro ASK1 Inhibitory Activity for 3*H*-Naphtho[1,2,3-*de*]quinoline-2,7-dione Derivatives

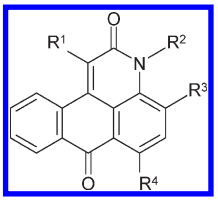

Compd	Structure				IC_{50}, μM
	R^1	R^2	R^3	R^4	
1	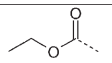	H	H	H	3
2	CH_3NH	CH_3	H	H	4,7
3	C_2H_5NH	CH_3	H	H	10
4	CH_3CO	H	H	H	15
5	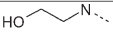	CH_3	H	H	25
6	PhCO	CH_3	H	H	35
7	CH_3CO	H	CH_3	H	35
8	CH_3CO	H	H	Cl	not active
9	CH_3CO	H	H	OH	not active
10	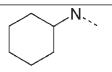	CH_3	H	Br	not active
11	H	CH_3	H	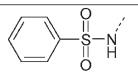	not active
12	H	CH_3	H	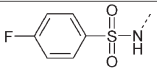	not active
13	H	CH_3	H	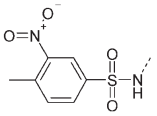	not active
14	H	CH_3	H	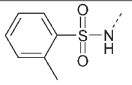	not active
15	H	CH_3	H	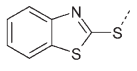	not active

there were no major changes observed. The rmsd plot for **1** demonstrates that no considerable disposition of the inhibitor occurs during MD simulation (Figure 2). The complex is stable during the calculation period with no detectable tendencies to dissociate.

The results of MD simulation allowed us to make the following deductions. Compound **1** occupies the ASK1 ATP-binding site,

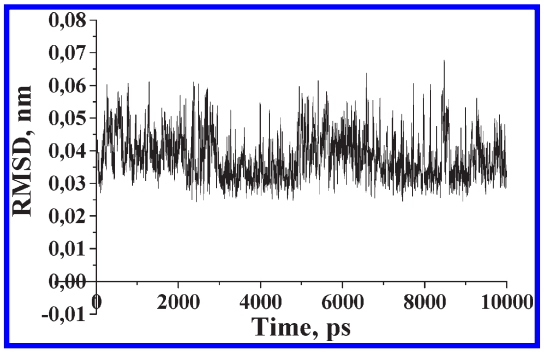

Figure 2. The rmsd of compound **1** in complex with ASK1 during MD simulation (smoothed by Savitzky−Golay method, 13 steps).

where it interacts with the hydrophobic pocket formed by the residues of the hinge region and adjacent residues of C-terminal and N-terminal lobes and forms hydrogen bonds with Gln756 and Val757. These interactions are present almost all the time during MD simulation. The hydrogen bond existence map calculated by GROMACS is represented in Figure 3.

The hydrogen-bond existence map shows long-term hydrogen bonds formed, on one hand, by carbonyl of ligand heterocyclic system and, on the other hand, by the amino group of Val757 (bond B) and the side chain amino group of Gln756 (bond C). The hydrogen bond between the ligand and Gln756 is disrupted at 5500 ps. The loss of this hydrogen bond was particularly compensated by the hydrogen bond between the carbonyl in the second position of the compound and hydroxyl group of Ser821 (bond A). At 7600 ps the hydrogen bond between the inhibitor and Gln756 is formed again.

The described hydrogen bond network correlates well with the energy of the complex (Figure 4). The average energy value of −110 kJ/mol reflects the presence of hydrogen bonds B and C. Significant slump of the energy curve is directly associated with the loss of hydrogen bond C. These data suggest an important role of this intermolecular hydrogen bond in the existence of the **1**−ASK1 complex.

Thus, using MD simulation we confirmed the formation of hydrogen bond between **1** and Val757. Also, the hydrogen bond with Gln756 in the hinge region of ASK1 ATP-binding pocket has been identified.

The residues Leu686, Val694, Ala707, Met754, Val757, Gly759, and Gly760 of the ASK1 ATP-binding site are involved in hydrophobic contacts with **1**. The major contributions to the hydrophobic interactions are provided by Leu686, Met754, and Leu810. These residues participate in the clamping of the inhibitor heterocyclic system and therefore in stabilization of the ligand in the active site. The MD snapshot characterizing the binding mode of **1** is represented in Figure 5.

Thus, in silico analysis of ASK1 complexes with inhibitors indicates that steric and hydrophobic effects contribute the most to the inhibitory activity of the compounds. The compounds providing hydrogen bonding capability with the hinge region of the ATP-binding site were shown to be potent inhibitors of ASK1. The results of biological tests allowed us to conclude that substituents R^1, R^3, and R^4 play a key role in ASK1 inhibitory activity for 3*H*-naphtho[1,2,3-*de*]quinoline-2,7-dione derivatives. These features can be used for the development of more potent inhibitors.

dx.doi.org/10.1021/jm200117h |*J. Med. Chem.* 2011, 54, 2680–2686

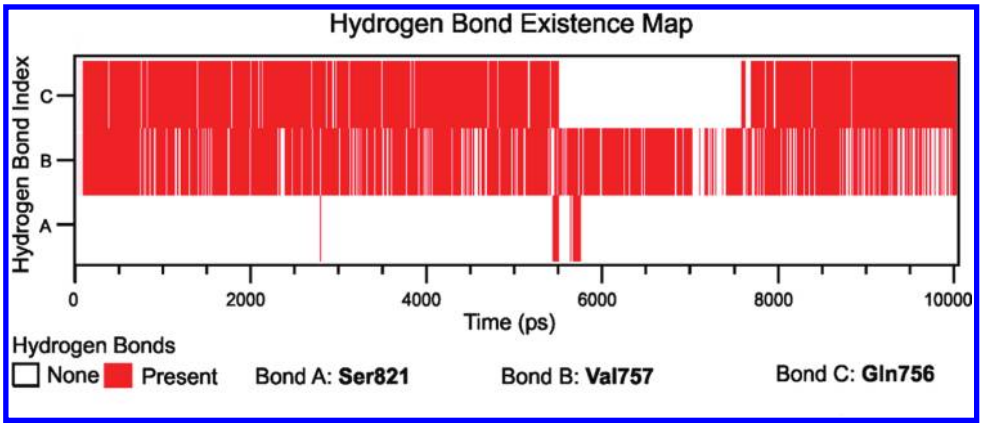

Figure 3. Hydrogen-bond existence map of **1**−ASK1 complex during a 10 ns MD simulation.

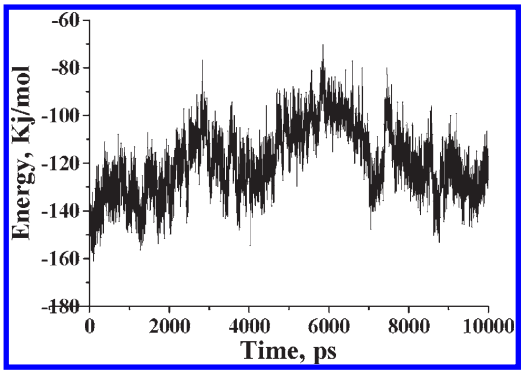

Figure 4. Sum of Coulomb and Lennard-Jones interaction energies for **1**−ASK1 complex during MD simulation (smoothed by Savitzky−Golay method, 13 steps).

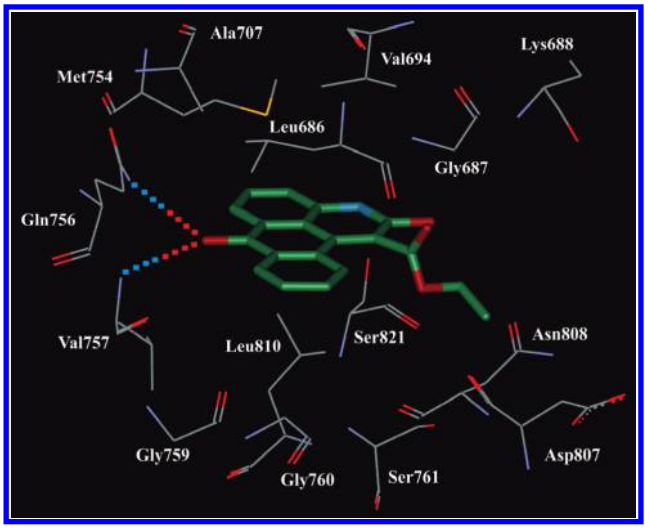

Figure 5. Binding mode of **1** in the active site of the ASK1 catalytic subunit. Hydrogen bonds are shown by the dotted lines.

CONCLUSIONS

Recent investigations of the ASK1 role in the functioning of the cellular signaling networks determined the connection between increased activity of the kinase and development of several pathologies. This provides the groundwork for the discovery of small-molecule inhibitors of ASK1 which may be used in medical practice. The goal of this study was to identify small-molecule inhibitors of protein kinase ASK1. Virtual screening allowed us to identify a small-molecule inhibitor of human protein kinase ASK1 among 3*H*-naphtho[1,2,3-*de*]quinoline-2,7-diones. In vitro experiments revealed that **1** inhibits ASK1 with a K_i of 500 nM. Inhibition of ASK1 by **1** is competitive with respect to the phosphodonor substrate ATP. According to the in silico modeling results, the mechanism of ASK1 inhibition involves the hydrogen bond formation between the carbonyl of compound **1** and the ASK1 hinge region. Our preliminary selectivity studies have demonstrated that **1** is a selective inhibitor of ASK1. These results strongly suggest that the core structure of this class of compounds can be used for the development of more potent and selective inhibitors of ASK1.

EXPERIMENTAL SECTION

Synthetic Chemistry. Starting materials and solvents were purchased from commercial suppliers and were used without further purification. ^{1}H NMR spectra were recorded on a Varian VXR 400 instrument at 400 MHz. Chemical shifts are described as parts per million (δ) downfield from an internal standard of tetramethylsilane, and spin multiplicities are given as s (singlet), d (doublet), dd (double doublet), t (triplet), q (quartet), or m (multiplet). HPLC−MS analysis was performed using the Agilent 1100 LC/MSD SL separations module and Mass Quad G1956B mass detector with electrospray ionization (+ve or −ve ion mode as indicated), and HPLC was performed using a Zorbax SB-C18, Rapid Resolution HT cartridge, 4.6 mm × 30 mm, 1.8 μm i.d. column (Agilent P/N 823975-902) at a temperature of 40 °C with gradient elution of 0−100% CH_3CN (with 1 mL/L HCOOH)/H_2O (with 1 mL/L HCOOH) at a flow rate of 3 mL/min and a run time of 2.8 min. Compounds were detected at 215 nm using a diode array G1315B detector. All tested compounds gave ≥95% purity as determined by this method. All purified synthetic intermediates gave ≥95% purity as determined by this method.

Ethyl 2,7-Dioxo-2,7-dihydro-3*H*-naphtho[1,2,3-*de*]quinoline-1-carboxylate (1). Compound **1** was prepared according to the method previously described.[17]

3-Methyl-1-(methylamino)-3*H*-naphtho[1,2,3-*de*]quinoline-2,7-dione (2), 3-Methyl-1-(ethylamino)-3*H*-naphtho[1,2,3-*de*]quinoline-2,7-dione (3), and 1-[(2-Hydroxyethyl)amino]-3-methyl-3*H*-naphtho[1,2,3-*de*]quinoline-2,7-dione (5). Compounds **2**, **3**, and **5** were prepared from 3-methylanthrapyridone-1-sulfonic acid sodium salt (**16**) that was synthesized accordingly to the original report.[18]

dx.doi.org/10.1021/jm200117h |*J. Med. Chem.* 2011, 54, 2680–2686

3-Methyl-1-(methylamino)-3*H*-naphtho[1,2,3-*de*]quinoline-2,7-dione (2). A solution of **16** (4.00 g, 0.011 mol) and sodium acetate (2.71 g, 0.033 mol) in methylamine (40% in H_2O, 400 mL) was heated to reflux for 30 h. The mixture was filtered. The resulting solid was taken up in H_2O (400 mL). The suspension was heated to reflux for 5 min, filtered, and dried to give **2** (2.97 g, 0.010 mol, 93%) as light brown needle crystals. LC−MS m/z 291 $[M + H^+]$, t_R = 0.97 min. ^{1}H NMR (DMSO-d_6) δ 2.76 (d, J = 5.5 Hz, 3H), 3.84 (s, 3H), 7.23−7.31 (m, 1H), 7.50 (t, J = 7.3 Hz, 1H), 7.55 (t, J = 7.8 Hz, 1H), 7.69−7.83 (m, 3H), 8.12 (d, J = 7.7 Hz, 1H), 8.25 (d, J = 7.7 Hz, 1H).

3-Methyl-1-(ethylamino)-3*H*-naphtho[1,2,3-*de*]quinoline-2,7-dione (3). A solution of **16** (4.00 g, 0.011 mol) and sodium acetate (2.71 g, 0.033 mol) in ethylamine (40% in H_2O, 400 mL) was heated to reflux for 30 h. The mixture was filtered. The resulting solids were dissolved in H_2O (400 mL). The suspension was heated to reflux for 5 min, filtered, and dried to give **3** (2.74 g, 0.093 mol, 82%) as light brown needle crystals. LC−MS m/z 305 $[M + H^+]$, t_R = 0.96 min. ^{1}H NMR (DMSO-d_6) δ 1.05 (t, J = 5.5 Hz, 3H), 3.85 (s, 3H), 7.20−7.31 (m, 1H), 7.51 (t, J = 7.3 Hz, 1H), 7.55 (t, J = 7.8 Hz, 1H), 7.67−7.82 (m, 3H), 8.12 (d, J = 7.7 Hz, 1H), 8.25 (d, J = 7.7 Hz, 1H).

1-[(2-Hydroxyethyl)amino]-3-methyl-3*H*-naphtho[1,2,3-*de*]quinoline-2,7-dione (5). A solution of **16** (4.00 g, 0.011 mol), sodium acetate (2.71 g, 0.033 mol), and ethanolamine (3.36 g, 0.055 mol) in H_2O (400 mL) was heated to reflux for 20 h. The mixture was filtered and solids were dried to give **5** (2.78 g, 0.009 mol, 79%) as yellow needle crystals. LC−MS m/z 321 $[M + H^+]$, t_R = 0.98 min. ^{1}H NMR (DMSO-d_6) δ 3.00−3.08 (m, 2H), 3.78 (t, J = 5.0 Hz, 2H), 3.86 (s, 3H), 3.75 (s, 1H, OH), 6.92 (t, J = 5.5 Hz, 1H), 7.51 (t, J = 7.5 Hz, 1H), 7.58 (t, J = 8.1 Hz, 1H), 7.75−7.82 (m, 2H), 8.00 (d, J = 8.1 Hz, 1H), 8.13 (d, J = 7.7 Hz, 1H), 8.26 (d, J = 8.1 Hz, 1H).

1-Benzoyl-3-methyl-3*H*-naphtho[1,2,3-*de*]quinoline-2,7-dione (6). A solution of 1-(methylamino)anthraquinone (9.49 g, 0.040 mol), sodium carbonate (424 mg, 4.0 mmol), and ethyl benzoylacetate (7.69 g, 0.100 mol) in xylene (36 mL) was stirred at 140−150 °C for 8 h. To complete the reaction, the ethanol and water formed during the reaction were removed by azeotropic distillation with xylene. The residue was cooled, and methanol (36 mL) was added. The mixture was stirred at 30 °C for 30 min, cooled, filtered, washed with methanol (36 mL), and dried to give **6** (13.31 g, 0.036 mol, 91%) as white needle crystals. LC−MS m/z 366 $[M + H^+]$, t_R = 1.02 min. ^{1}H NMR (DMSO-d_6) δ 3.78 (s, 3H), 7.49−7.60 (m, 3H), 7.62−7.72 (m, 2H), 7.78 (d, J = 8.1 Hz, 1H), 7.90−8.05 (m, 4H), 8.22 (d, J = 7.4 Hz, 1H), 8.36 (d, J = 7.8 Hz, 1H).

1-Acetyl-6-hydroxy-3*H*-naphtho[1,2,3-*de*]quinoline-2,7-dione (9). A solution of 1-amino-4-hydroxyanthraquinone (9.57 g, 0.040 mol), sodium carbonate (424 mg, 4.0 mmol), and ethyl acetoacetate (13.01 g, 0.100 mol) in xylene (36 mL) was stirred at 140−150 °C for 8 h. To complete the reaction, the ethanol and water formed during the reaction were removed by azeotropic distillation with xylene. The residue was evaporated, and methanol (12 mL) was added. The mixture was stirred at 30 °C for 30 min, cooled, filtered, washed with methanol (12 mL), and dried to give **9** (9.38 g, 0.031 mol, 77%) as white crystals. LC−MS m/z 306 $[M + H^+]$, t_R = 0.87 min. ^{1}H NMR (DMSO-d_6) δ 2.68 (s, 3H), 7.33 (d, J = 8.8 Hz, 1H), 7.66−8.02 (m, 4H), 8.51 (d, J = 7.4 Hz, 1H), 12.69 (s, 1H, OH), 13.60 (s, 1H, NH).

1-Acetyl-3*H*-naphtho[1,2,3-*de*]quinoline-2,7-dione (4), 1-Acetyl-4-methyl-3*H*-naphtho[1,2,3-*de*]quinoline-2,7-dione (7), and 1-Acetyl-6-chloro-3*H*-naphtho[1,2,3-*de*]quinoline-2,7-dione (8). Compounds **4**, **7**, and **8** were prepared from appropriate 1-aminoanthraquinones according to the method described for above-mentioned compound **9**.

1-Acetyl-3*H*-naphtho[1,2,3-*de*]quinoline-2,7-dione (4). Yield 85% (white powder). LC−MS m/z 290 $[M + H^+]$, t_R = 0.91 min. ^{1}H NMR (DMSO-d_6) δ 2.68 (s, 3H), 7.66−7.84 (m, 4H), 7.87 (d, J = 8.1 Hz, 1H), 8.09 (d, J = 7.2 Hz, 1H), 8.39 (d, J = 7.7 Hz, 1H), 12.60 (s, 1H, NH).

1-Acetyl-4-methyl-3*H*-naphtho[1,2,3-*de*]quinoline-2,7-dione (7). Yield 83% (white powder). LC−MS m/z 304 $[M + H^+]$, t_R = 0.95 min. ^{1}H NMR (DMSO-d_6) δ 2.60 (s, 3H), 2.67 (s, 3H), 7.60 (d, J = 7.7 Hz, 1H), 7.69−7.80 (m, 2H), 7.86 (d, J = 7.5 Hz, 1H), 8.01 (d, J = 7.6 Hz, 1H), 8.36 (d, J = 7.5 Hz, 1H), 11.75 (s, 1H, NH).

1-Acetyl-6-chloro-3*H*-naphtho[1,2,3-*de*]quinoline-2,7-dione (8). Yield 89% (white powder). LC−MS m/z 324 $[M + H^+]$, t_R = 0.98 min. ^{1}H NMR (DMSO-d_6) δ 2.67 (s, 3H), 7.63 (d, J = 8.8 Hz, 1H), 7.74−7.88 (m, 4H), 8.27 (d, J = 7.2 Hz, 1H), 12.64 (s, 1H, NH).

6-Bromo-1-(cyclohexylamino)-3-methyl-3*H*-naphtho[1,2,3-*de*]quinoline-2,7-dione (10). Compound **10** was prepared from 1-(cyclohexylamino)-3-methyl-3*H*-naphtho[1,2,3-*de*]quinoline-2,7-dione (**17**) that was synthesized by the method previously described.[18] Bromine (240 mg, 1.5 mmol) in acetic acid (5 mL) was added dropwise over 10 min to a solution of **17** (537 mg, 1.5 mmol) in acetic acid (5 mL). After 1 h, the volatiles were removed under reduced pressure and the residual solid was recrystallized from ethanol to give **10** (466 mg, 1.06 mmol, 71%). LC−MS m/z 438 $[M + H^+]$, t_R = 1.29 min. ^{1}H NMR (DMSO-d_6) δ 0.98−1.86 (m, 10H), 3.22−3.36 (m, 1H), 6.31 (d, J = 9.9 Hz, 1H, NH), 7.53 (t, J = 7.4 Hz, 1H), 7.65 (d, J = 9.0 Hz, 1H), 7.71 (t, J = 7.4 Hz, 1H), 7.76 (d, J = 8.8 Hz, 1H), 8.10−8.23 (dd, 2H).

General Procedures for the Synthesis of Compounds 11−14. Compounds **11**−**14** were prepared from amino-3-methyl-3*H*-naphtho[1,2,3-*de*]quinoline-2,7-dione (**18**) that was synthesized according to the method previously described.[14] A solution of **18** (276 mg, 1.0 mmol) in pyridine (2 mL) was treated with the appropriate sulfonyl chloride (1.0 mmol), and the mixture was stirred at room temperature for 24 h. The reaction mixture was diluted with water (10 mL) and filtered. The solid was washed with H_2O (5 mL), isopropyl alcohol (IPA) (2 mL) and air-dried.

***N*-(3-Methyl-2,7-dioxo-2,7-dihydro-3*H*-naphtho[1,2,3-*de*]quinolin-6-yl)benzenesulfonamide (11).** Yield 89% (white powder). LC−MS m/z 417 $[M + H^+]$, t_R = 1.04 min. ^{1}H NMR (DMSO-d_6) δ 3.74 (s, 3H), 7.50−7.64 (m, 3H), 7.77 (t, J = 7.7 Hz, 1H), 7.85−7.97 (m, 4H), 7.97−8.09 (m, 2H), 8.40 (d, J = 7.8 Hz, 1H), 8.52 (d, J = 8.2 Hz, 1H), 12.83 (s, 1H, NH).

4-Fluoro-*N*-(3-methyl-2,7-dioxo-2,7-dihydro-3*H*-naphtho[1,2,3-*de*]quinolin-6-yl)benzenesulfonamide (12). Yield 93% (white powder). LC−MS m/z 435 $[M + H^+]$, t_R = 1.06 min. ^{1}H NMR (DMSO-d_6) δ 3.74 (s, 3H), 7.30 (t, J = 8.4 Hz, 2H), 7.77 (t, J = 7.7 Hz, 1H), 7.83−7.91 (m, 2H), 7.96−8.07 (m, 4H), 8.37 (d, J = 7.9 Hz, 1H), 8.50 (d, J = 8.2 Hz, 1H), 12.80 (s, 1H, NH).

4-Methyl-*N*-(3-methyl-2,7-dioxo-2,7-dihydro-3*H*-naphztho[1,2,3-*de*]quinolin-6-yl)-3-nitrobenzenesulfonamide (13). Yield 91% (yellow powder). LC−MS m/z 476 $[M + H^+]$, t_R = 1.08 min. ^{1}H NMR (DMSO-d_6) δ 3.74 (s, 3H), 7.66 (d, J = 8.1 Hz, 1H), 7.66 (t, J = 7.5 Hz, 1H), 7.81−7.91 (m, 2H), 7.96−8.07 (m, 2H), 8.11 (d, J = 7.8 Hz, 1H), 8.37 (d, J = 7.8 Hz, 1H), 8.46 (s, 1H), 8.49 (d, J = 7.8 Hz, 1H), 12.88 (s, 1H, NH).

2-Methyl-*N*-(3-methyl-2,7-dioxo-2,7-dihydro-3*H*-naphtho[1,2,3-*de*]quinolin-6-yl)benzenesulfonamide (14). Yield 88% (white powder). LC−MS m/z 431 $[M + H^+]$, t_R = 1.09 min. ^{1}H NMR (DMSO-d_6) δ 2.64 (s, 3H), 3.70 (s, 3H), 7.15−7.65 (m, 3H), 7.65−8.06 (m, 5H), 8.11 (d, J = 7.8 Hz, 1H), 8.42 (d, J = 7.8 Hz, 1H), 8.50 (d, J = 7.8 Hz, 1H), 13.05 (s, 1H, NH).

6-(1,3-Benzothiazol-2-ylthio)-3-methyl-3*H*-naphtho[1,2,3-*de*]quinoline-2,7-dione (15). Compound **15** was prepared from 6-bromo-3-methyl-3*H*-naphtho[1,2,3-*de*]quinoline-2,7-dione **19** that was synthesized according to the method previously described.[19] A solution of **19** (408 mg, 1.2 mmol), 2-mercaptobenzothiazole (200 mg, 1.2 mmol), and triethylamine (121 mg, 1.2 mmol) in DMF (5 mL) was heated at 100 °C for 48 h. The mixture was diluted with H_2O (15 mL)

and filtered. The solid was washed with IPA (10 mL) and dried to provide **15** (425 mg, 1.0 mmol, 83%). LC−MS m/z 427 [M + H$^+$], t_R = 1.16 min. ^{1}H NMR (DMSO-d_6) δ 3.71 (s, 3H), 7.49−7.68 (m, 3H), 7.73−7.84 (m, 3H), 7.67 (t, J = 7.4 Hz, 1H), 8.08 (d, J = 7.9 Hz, 2H), 8.34 (d, J = 7.7 Hz, 1H), 8.48 (d, J = 8.2 Hz, 1H).

Receptor Preparation for Flexible Docking. The crystal structure of human protein kinase ASK1 was obtained from the Brookhaven Protein Data Bank (PDB code 2CLQ).[20] The catalytic subunit has been extracted from the PDB file, and the staurosporine has been removed from the ASK1−staurosporine complex. In the crystal structure some amino acids side chain atoms are missing. The homology model of ASK1 has been built using the SWISS-MODEL workspace.[21]

A receptor molecule has been minimized in water with the GROMACS molecular dynamics simulation package (GROMACS force field, steepest descent algorithm, 1000 steps, em_tolerance = 100, em_step = 0.001). The partial atom charges of the receptor molecule were taken from the Amber force field. Active site spheres were calculated with DOCK sphgen software. The spheres with positions outside the ATP-binding site were deleted manually. Connolly MS and Grid programs from the DOCK package were used to generate receptor Connolly surface and energy grids. Surface and grid calculations were performed with parameter settings detailed in ref 22. The grid spacing was set to 0.3.

Ligand Database Processing. Calculations of ligand geometry were performed using YFF force field described in ref 23. Partial atomic charges of the ligands were calculated with the Kirchhoff method.[24]

Flexible Docking. DOCK program has been used for receptor−ligand flexible docking. DOCK input parameters have been set as described previously.[22] In our virtual screening experiments the "multiple anchors" parameter was set as follows: the minimum of heavy atoms in the anchor was set to 6; the maximum number of orientations was set to 1000; the "all atoms" model has been chosen. 172 compounds with scores from −50 to −90 kcal/mol have been taken for the kinase assay analysis.

The duration of the virtual screening experiment was around 9 days. We used 21 processors, 3 GHz.

The structures were visualized using the program ViewerLite, version 4.2.[25]

Molecular Dynamics. The starting position of the ligand in the active site of the receptor was generated with the DOCK software package. GROMACS package and GROMOS96 force field were used for experiments of MD.[26] Energy minimization of molecular complexes was carried out in explicit water environment with steepest descent energy minimization algorithm for 1000 relaxation steps. The minimized structure proceeded to position restrain dynamics, and the relaxation time was 20 ps. On the next stage an MD of 10 ns was calculated. The integration of the equations of motion was performed using the leapfrog algorithm.[27] In the MD simulation, the canonical (NVT) ensemble was used. This ensemble involves keeping the number of particles (N), system volume (V), and temperature (T) constant/conserved. Therefore, no pressure coupling was used. V-rescale thermostat at 300 K was taken to control the simulation temperature. For electrostatics treatment, particle mesh Ewald algorithm was applied.[28]

Biochemical Testing. Enzyme activity of human protein kinases ASK1, Aurora A, ROCK1, HGFR, FGFR1, Tie2, JNK3, and CK2 was determined using in vitro kinase assay (γ-^{32}P-ATP method). Each reaction mixture contained 6 μL of buffer solution (25 mM MOPS, pH 7.2, 2.5 mM EGTA, 2.5 mM EDTA, 0.5 mM DTT, 0.25 mg/mL BSA, 20 mM β-glycerophosphate), 3 μL of substrate solution (MBP, Kemptide, Long S6 kinase substrate peptide, KKKSPGEYVNIEFG, IGF-IRtide (12-527), TK substrate 2, JNK3tide, or RRRDDDSDDD for each kinase, respectively) (5.0 μg/μL), 0.3 μL of enzyme (protein kinase catalytic subunit, 0.1 μg/μL ≈ 32 mU/μL) ("Upstate/Millipore"), and 10.25 μL of H_2O. The reaction mixture (total volume of 19 μL) was quickly added to 1.5 mL tubes at room temperature.

The stock solutions of inhibitors were prepared in DMSO, and the concentration of inhibitor was 1 mM. The concentration of DMSO in the reaction did not exceed 3%. Then 1 μL of inhibitor solution in DMSO was added to each tube and mixed by pipetting. ATP solution was prepared separately. For each sample 0.05 mCi γ-[P^{32}]ATP was taken (specific activity of 100 μCi/μM).

The total concentration of labeled and unlabeled ATP was 100 μM. The reaction was started with addition of ATP solution (150 μM ATP, 30 mM $MgCl_2$, 15 mM MOPS, pH 7.2). The time of reaction was 20 min at 30 °C. The reaction was stopped by adding 20 μL of 0.5 M orthophosphoric acid. Then the reaction mixture was loaded on the 20 mm filter disks of the cellulose phosphate paper ("Whatman", Great Britain). Filters were washed three times with 0.075 M orthophosphoric acid at room temperature and dried. For detection of products, dried filters were counted by PerkinElmer model Tri-Carb 2800-TR liquid scintillation analyzer. Then 1 μL of DMSO was added to the reaction volume instead of the inhibitor stock solution for a positive control.

AUTHOR INFORMATION

Corresponding Author

*Phone/Fax: +38 044 522 2458. E-mail: yarmoluksm@gmail.com.

ACKNOWLEDGMENT

This work was supported by the National Academy of Sciences of Ukraine (Grant 0107U000337).

ABBREVIATIONS USED

ASK1, apoptosis signal-regulating kinase 1; polyQ, polyglutamine; ROS, reactive oxygen species; Aβ, amyloid β; LPS, lipopolysaccharide; CK2, protein kinase CK2; JNK3, c-Jun N-terminal kinase 3; ROCK1, Rho-associated protein kinase 1; FGFR1, fibroblast growth factor receptor 1; HGFR, hepatocyte growth factor receptor; Tie2, TEK tyrosine kinase, endothelial; MD, molecular dynamics; IPA, isopropyl alcohol

REFERENCES

(1) Nishitoh, H.; Matsuzawa, A.; Tobiume, K.; Saegusa, K.; Takeda, K.; Inoue, K.; Hori, S.; Kakizuka, A.; Ichijo, H. ASK1 is essential for endoplasmic reticulum stress-induced neuronal cell death triggered by expanded polyglutamine repeats. *Genes Dev.* **2002**, *16*, 1345–1355.

(2) Hashimoto, Y.; Niikura, T.; Chiba, T.; Tsukamoto, E.; Kadowaki, H.; Nishitoh, H.; Yamagishi, Y.; Ishizaka, M.; Yamada, M.; Nawa, M.; Terashita, K.; Aiso, S.; Ichijo, H.; Nishimoto, I. The cytoplasmic domain of Alzheimer's amyloid-beta protein precursor causes sustained apoptosis signal-regulating kinase 1/c-Jun NH2-terminal kinase-mediated neurotoxic signal via dimerization. *J. Pharmacol. Exp. Ther.* **2003**, *306*, 889–902.

(3) Nishitoh, H.; Kadowaki, H.; Nagai, A.; Maruyama, T.; Yokota, T.; Fukutomi, H.; Noguchi, T.; Matsuzawa, A.; Takeda, K.; Ichijo, H. ALS-linked mutant SOD1 induces ER stress- and ASK1-dependent motor neuron death by targeting Derlin-1. *Genes Dev.* **2008**, *22*, 1451–1464.

(4) Yamamoto, E.; Dong, Y. F.; Kataoka, K.; Yamashita, T.; Tokutomi, Y.; Matsuba, S.; Ichijo, H.; Ogawa, H.; Kim-Mitsuyama, S. Olmesartan prevents cardiovascular injury and hepatic steatosis in obesity and diabetes, accompanied by apoptosis signal regulating kinase-1 inhibition. *Hypertension* **2008**, *52*, 573–580.

(5) Hikoso, S.; Ikeda, Y.; Yamaguchi, O.; Takeda, T.; Higuchi, Y.; Hirotani, S.; Kashiwase, K.; Yamada, M.; Asahi, M.; Matsumura, Y.; Nishida, K.; Matsuzaki, M.; Hori, M.; Otsu, K. Progression of heart

failure was suppressed by inhibition of apoptosis signal-regulating kinase 1 via transcoronary gene transfer. *J. Am. Coll. Cardiol.* **2007**, *50*, 453–462.

(6) Matsuzawa, A.; Saegusa, K.; Noguchi, T.; Sadamitsu, C.; Nishitoh, H.; Nagai, S.; Koyasu, S.; Matsumoto, K.; Takeda, K.; Ichijo, H. ROS-dependent activation of the TRAF6-ASK1-p38 pathway is selectively required for TLR4-mediated innate immunity. *Nat. Immunol.* **2005**, *6*, 587–592.

(7) Chibon, F.; Mariani, J.; Derre, A.; Mairal, J. M.; Condre, L.; Guillou, X.; Sastre, F.; Pedeteuor, F.; Aurias, A. ASK1 (MAP3K5) as a potential therapeutic target in malignant fibrous histiocytomas with 12q14-q15 and 6q23 amplifications. *Genes, Chromosomes Cancer* **2004**, *40*, 32–37.

(8) Uchikawa, O; Sakai, N.; Terao, Y.; Suzuki, H. WO 2008016131 A1, 2008; EP 2058309 A1, 2009; US 20100029619, 2010.

(9) Volynets, G. P.; Bdzhola, V. G.; Kukharenko, O. P.; Yarmoluk, S. M. Identification of ASK1 small-molecule inhibitors. *Ukr. Biokhim. Zh.* **2010**, *82*, 41–50.

(10) Okamoto, M.; Saito, N.; Kojima, H.; Okabe, T.; Takeda, K.; Ichijo, H.; Furuya, T.; Nagano, T. Identification of novel ASK1 inhibitors using virtual screening. *Bioorg. Med. Chem.* **2011**, *19*, 486–489.

(11) Kitchen, D. B.; Decornez, H.; Furr, J. R.; Bajorath, J. Docking and scoring in virtual screening for drug discovery: methods and applications. *Nat. Rev Drug Discovery* **2004**, *3*, 935–949.

(12) Stoichet, B. K.; Stroud, R. M.; Santi, D. V.; Kuntz, I. D.; Perry, K. M. Structure-based discovery of inhibitors of thymidylate synthase. *Science* **1993**, *259*, 1445–1450.

(13) Bodian, D. L.; Yamasaki, R. B.; Buswell, R. L.; Stearns, J. F.; White, J. M.; Kuntz, I. D. Inhibition of the fusion-inducing conformational change of influenza hemagglutinin by benzoquinones and hydroquinones. *Biochemistry* **1993**, *32*, 2967–2978.

(14) Ring, C. S.; Sun, E.; McKerrow, J. H.; Lee, G. K.; Rosenthal, P. J.; Kuntz, I. D.; Cohen, F. E. Structure-based inhibitor design by using protein models for the development of antiparasitic agents. *Proc. Natl. Acad. Sci. U.S.A.* **1993**, *90*, 3583–3587.

(15) Ewing, T. J.; Makino, S.; Skillman, A. G.; Kuntz, I. D. DOCK 4.0: search strategies for automated molecular docking of flexible molecule databases. *J. Comput.-Aided Mol. Des.* **2001**, *15*, 411–428.

(16) We used a database of commercially available compounds (Otava Ltd., http://www.otavachemicals.com/).

(17) Bu, X.; Deady, L. W.; Finlay, G. J.; Baguley, B. C.; Denny, W. A. Synthesis and cytotoxic activity of 7-oxo-7*H*-dibenz[*f,ij*]isoquinoline and 7-oxo-7*H*-benzo[*e*]perimidine derivatives. *J. Med. Chem.* **2001**, *44*, 2004–2014.

(18) Kazankov, M. V.; Putsa, G. I. Synthesis of anthradipyridone derivatives. *Chem. Heterocycl. Compd. (N. Y., NY, U. S.)* **1973**, *9*, 763–767.

(19) Allen, C. F. H.; Wilson, C. V. Nitroanthrapyridones. *J. Org. Chem.* **1945**, *10*, 594–602.

(20) Bunkoczi, G.; Salah, H.; Filippakopoulos, P.; Fedorov, O.; Müller, S.; Sobott, F.; Parker, S. A.; Zhang, H.; Min, W.; Turk, B. E.; Knapp, S. Structural and functional characterization of the human protein kinase ASK1. *Structure* **2007**, *15*, 1215–1226.

(21) Homology model of ASK1 was built using the SWISS-MODEL workspace (http://swissmodel.expasy.org/).

(22) Bursulaya, B. D.; Totrov, M.; Abagyan, R.; Brooks, C. L., III. Comparative study of several algorithms for flexible ligand docking. *J. Comput.-Aided Mol. Des.* **2003**, *17*, 755–763.

(23) Yakovenko, O. Ya.; Oliferenko, A. A.; Golub, A. G.; Bdzhola, V. G.; Yarmoluk, S. M. The new method of distribution integrals evaluations for high throughput virtual screening. *Ukr. Bioorg. Acta* **2007**, *1*, 52–62.

(24) Yakovenko, O. Ya.; Oliferenko, A. A.; Bdzhola, V. G.; Palyulin, V. A.; Zefirov, N. S. Kirchhoff atomic charges fitted to multipole moments: implementation for a virtual screening system. *J. Comput. Chem.* **2008**, *29*, 1332–1343.

(25) The structures were visualized using the program ViewerLite, version 4.2. (Accelrys Inc., http://www.accelrys.com).

(26) Oostenbrink, C.; Villa, A.; Mark, A. E.; Van Gunsteren, W. F. A biomolecular force field based on the free enthalpy of hydration and solvation: the GROMOS force-field parameter sets 53A5 and 53A6. *J. Comput. Chem.* **2004**, *25* (13), 1656–1676.

(27) Hockney, R. W.; Goel, S. P.; Eastwood, J. Quiet high resolution computer models of a plasma. *J. Comput. Phys.* **1974**, *14*, 148–158.

(28) Darden, T.; Perera, L.; Li, L.; Pedersen, L. New tricks for modelers from the crystallography toolkit: the particle mesh Ewald algorithm and its use in nucleic acid simulations. *Structure* **1999**, *7*, 55–60.